

## SIMULATION OF FLUID PHASE EQUILIBRIA IN SQUARE-WELL FLUIDS: FROM THREE TO TWO DIMENSIONS

Horst L. VÖRTLER

*Molecular Dynamics and Computer Simulation Research Group, Institute of Theoretical Physics, University of Leipzig, Postfach 100920, 04009 Leipzig, Germany;  
e-mail: horst.voertler@physik.uni-leipzig.de*

Received January 2, 2008

Accepted April 9, 2008

Published online May 2, 2008

*Dedicated to Professor William R. Smith on the occasion of his 65th birthday.*

We study the influence of geometric restrictions on vapour/liquid coexistence properties and critical data of square-well fluids. Starting with three-dimensional bulk systems, we model the confinement by slit-like pores with decreasing slit widths arriving finally at planar (two-dimensional) fluid layers. For both bulk and confined fluids, we use a uniform approach performing series of canonical ensemble Monte Carlo simulations with Widom-like (virtual) particle insertions to estimate chemical potential versus density isotherms. By estimating the corresponding vapour/liquid coexistence densities using a Maxwell-like equal area rule for the subcritical chemical potential isotherms, we are able to study the influence of the confinement not only on chemical potentials but also on the coexistence properties. Critical point data are calculated from the coexistence densities by means of scaling relations. In particular, we study the change of the critical temperature and critical density varying the slit width and including the two- and three-dimensional bulk fluids as limiting cases. While the difference between the bulk and the slit critical temperature is found to decay exponentially with an exponent reciprocal to a linear function in the slit width, no comparable simple relation describing the influence of the confinement on the critical density is found.

**Keywords:** Square-well potential; Chemical potential; Phase equilibrium; Monte Carlo simulation; Critical point.

The study of the influence of geometric restrictions on the phase equilibrium properties of basic fluid models by statistical mechanical and simulation methods provides important contributions to a molecular-based understanding of surface and interfacial phenomena, such as adsorption and capillary condensation of fluids interacting with biologically active surfaces (membranes), and fluids confined in microporous media (zeolites).

Inhomogeneous fluids have been extensively studied during the last decades by diverse integral equations, perturbation theory, and computer simulation methods (for comprehensive reviews of recent work on confined fluids, see e.g. Evans<sup>1</sup> and Gelb et al.<sup>2</sup>).

Recently, we introduced a method to study phase equilibria and critical properties of fluids that combines canonical Monte Carlo (MC) simulations of chemical potentials by particle insertion methods with the thermodynamic integration of the simulated subcritical chemical potential versus density isotherms by means of a Maxwell-like equal area rule<sup>3</sup>. This approach is conceptually simple and requires only the implementation of Widom-like (virtual) particle insertion in existing canonical simulation codes. It provides an alternative route to phase equilibria simulations in the grand canonical ensemble and to Gibbs ensemble simulations.

We proved the ability of this approach to estimate reliable chemical potential isotherms and phase equilibrium properties for bulk and confined square-well fluids<sup>3</sup>, and we discussed to what extent finite size effects affect the results<sup>4</sup>. This approach was also applied to calculate phase equilibria of primitive water models, where hydrogen bonding is described by square-well interactions<sup>5,6</sup>.

Based on this approach, in this paper we study systematically the influence of geometrical restrictions on phase coexistence properties and critical properties of square-well fluids.

We study the square-well fluid mainly for two reasons:

1. It is one of the simplest molecular fluid models that is able to represent the realistic fluid phase equilibria of real simple liquids.
2. It is a basic intermolecular potential, which is involved in molecular models of several classes of more complex molecular liquids, such as polymers<sup>7</sup> or aqueous liquids<sup>8</sup>.

While the bulk properties of square-well fluids are well understood (for a recent summary of phase equilibrium properties, see ref.<sup>9</sup>), the knowledge of fluid phase equilibria of square-well fluids in simple confinements is surprisingly poor. Particularly, for fluids confined in hard slit-like pores – including planar monolayers – only few computer simulation data are available<sup>3,4,10</sup>.

In order to model the increasing influence of the confinement on the bulk properties, we start with a three-dimensional bulk system and model the confinement by a sequence of slit-like pores with decreasing slit width, arriving finally at a planar (two-dimensional) fluid monolayer. Particularly, we study the shift of the critical temperature under confinement.

The paper is organized as follows. In the second section we describe the fluid models and the methodology used, including some technical details. In the third section we present our results for phase equilibria of bulk and confined square-well systems, such as coexistence densities and critical data. This is followed by a discussion of the critical point shift and comparison of our results with existing literature results. Finally, as a summary of our studies, we draw some general conclusions concerning the confinement influence on phase equilibria and critical properties.

#### SYSTEMS UNDER CONSIDERATION AND METHODS USED

In this paper we consider a square-well fluid with the intermolecular potential model described by

$$u(r) = \begin{cases} \infty & \text{for } r \leq \sigma \\ -\varepsilon & \text{for } \sigma < r \leq \lambda\sigma \\ 0 & \text{for } r > \lambda\sigma \end{cases} \quad (1)$$

where  $\sigma$  is the diameter of the particles and  $\varepsilon$  and  $\lambda$  describe the depth and width of the potential well, respectively. Throughout the paper we set  $\lambda = 1.5$  and use reduced units

$$r^* = r/\sigma \quad u^* = u/\varepsilon \quad T^* = kT/\varepsilon \quad (2)$$

for distance, energy, and temperature, respectively. We study both normal three-dimensional bulk square-well fluids and geometrically restricted fluids confined to slit-like pores with diverse widths  $L$  reaching from  $L = 2.5\sigma$  to  $10\sigma$ , and we include as limiting case  $L = 1\sigma$ , i.e., planar layers (two-dimensional arrangements) of square-well particles. We perform standard canonical MC simulation<sup>11,12</sup> using for the bulk fluid the usual cubic simulation cell with periodic boundary conditions in three dimensions ( $x$ ,  $y$ ,  $z$ ) in space. For the confined fluid a simulation box is used of cross-sectional area  $A$  with lengths  $\ell_x = \ell_y \equiv \ell$  in the  $x$ - and  $y$ -directions, and of height  $L$  in  $z$ -direction corresponding to the wall separation distance of the slit. In the  $x$ - and  $y$ -directions, periodic boundary conditions are applied. We generate the corresponding Markov chains of configurations by performing random trial displacements of the particles, and we measure the chemical potential by inserting (virtually) test particles in the simulated configurations. We applied the standard Widom test particle method<sup>13</sup>. The

efficiency of the method suffices for our calculations, because the densities in the gas/liquid transition range of interest are not extremely high. For recent variants of insertion methods and discussion of the efficiency problem, see, e.g.<sup>5,6,14-16</sup>.

According to Widom<sup>13,17</sup>, the excess chemical potential over the ideal gas value for both homogeneous and inhomogeneous fluids with an intermolecular potential  $U_N(\vec{r}^N)$  may be written in the form

$$\beta\mu^{\text{ex}} = -\ln\left(\left\langle \exp[-\beta\Delta W_{N+1,N}] \right\rangle_N\right)_{r_{N+1}} \quad (3)$$

where  $\beta = 1/kT$ , and  $W_N(\vec{r}^N) = U_N(\vec{r}^N) + U_N^{\text{exp}}(\vec{r}^N)$  is the total potential energy of the fluid in an external potential  $U_N^{\text{exp}}(\vec{r}^N)$ . In our case the external potential

$$U_N^{\text{ext}}(z) = \begin{cases} 0 & \text{for } |z| \leq (L - \sigma)/2 \\ \infty & \text{for } |z| > (L - \sigma)/2 \end{cases} \quad (4)$$

models the hard walls of the confining slit of width  $L$ , i.e., the centers of the particles can freely move in a slit of width  $L - \sigma$ .

The canonical MC average  $\langle \exp[-\beta\Delta W_{N+1,N}] \rangle_N$  of the difference of the Boltzmann factors between systems with  $N$  and  $N + 1$  particles in Eq. (3) is measured by virtual insertions of test particles in the  $N$ -particle system at random positions in the usual way<sup>12</sup>. The total chemical potential of the fluid is the sum of the ideal gas contribution and the excess chemical potential (3) given by

$$\beta\mu = \ln(\rho\sigma^3) + \beta\mu^{\text{ex}} \quad (5)$$

where  $\rho = N/V$  is the number density of the fluid.

Typically the Markov chains generated at subcritical temperatures consist of  $10^6$ – $10^8$  MC translation moves per particle. The same number of virtual particle insertion attempts are performed to measure the chemical potential. The longest chains are required in the density range between the equilibrium vapour and liquid densities, where van der Waals-like loops in the chemical potential isotherms occur.

The relative error of the simulated chemical potentials, found by means of the block average method<sup>18</sup>, is of the order of  $(1-3) \times 10^{-3}$ . More technical details about the chemical potential simulations can be found in our

previous paper<sup>4</sup>, which discusses in detail also the influence of the system size on the results.

In order to calculate the coexistence densities, we use smoothed chemical potential  $\mu$  versus density  $\rho$  isotherms, obtained by fitting the simulation results to analytical polynomials of the form

$$\beta\mu = \sum_{i=0}^k b_i (\rho\sigma^3)^{i-2} \quad (6)$$

with adjustable parameters  $b_i$  and  $k = 11$ . The coexistence densities we obtain from the smoothed isotherms by means of a Maxwell-like equal-area integration, by numerically implementing the condition of equal chemical potentials of the coexisting phases, in the same way as discussed in our previous papers<sup>3,5</sup>. In order to obtain the critical temperature  $T_c^*$  and the critical density  $\rho_c$ , we use well-known scaling relations, which are valid in the vicinity of the critical point. We use a nonlinear regression procedure to fit the coexistence densities to the scaling expression

$$\rho_{\ell/v} = \rho_c + C_2 (1 - T^*/T_c^*) \pm 0.5B_0 (1 - T^*/T_c^*)^\beta; \quad T < T_c \quad (7)$$

based on a Wegner expansion<sup>19</sup>, where – following the common practice – higher order terms were neglected<sup>20,21</sup>. The constants  $C_2$ ,  $B_0$  and the critical exponent  $\beta$  are treated as adjustable parameters.

## PHASE EQUILIBRIA OF BULK AND CONFINED SQUARE-WELL SYSTEMS

### *Vapour/Liquid Coexistence Properties*

As discussed above, the first step in our methodology to estimate coexistence properties is to simulate  $\mu$  versus  $\rho$  isotherms by means of canonical MC with (virtual) test particle insertions in the subcritical temperature range for both the bulk and confined square-well fluids. For the purposes of this paper, we have simulated new  $\mu(\rho)$  isotherms for fluids confined to slit-like pores with wall separation distances  $L = \{2.5\sigma, 6.0\sigma, 10.0\sigma\}$  and corresponding particle numbers of  $N = \{392, 500, 567\}$ . We have also studied a set of smaller systems for the same slit widths with particle numbers  $N = \{162, 256, 343\}$  to explore system size effects. Additionally, we have used

existing simulation data for bulk fluids and slits with width  $L = 4\sigma$  and planar monolayers ( $L = 1\sigma$ ), reported in our previous papers<sup>3,4</sup>.

Figure 1 presents two typical subcritical isotherms, showing one isotherm for the smallest slit ( $L = 2.5\sigma$ ,  $T^* = 0.75$ ,  $N = 392$ ) and one for the widest slit ( $L = 10.0\sigma$ ,  $T^* = 1.05$ ,  $N = 567$ ), including both the rough simulation data and the smoothed curves. The van der Waals-like loops connecting the stable equilibrium vapour phase with the stable equilibrium liquid phase are evident. For comparison, we show for both slit widths the same isotherms simulated with smaller numbers of particles, i.e., in the case of  $L = 2.5\sigma$  with  $N = 162$  and in the case of  $L = 10.0\sigma$  with  $N = 343$ . We observe a significant number dependence of the chemical potentials in the loop range (i.e., a smaller loop for the larger system), but nearly no number dependence in the stable gaseous and liquid density ranges. This is in agreement with general considerations<sup>22</sup>, and results for Lennard–Jones systems<sup>23,24</sup>, and our recent systematic study of the particle number dependence of  $\mu(\rho)$  loops of square-well fluids<sup>4</sup> where, with increasing number of particles, in general a shrinking of the loops is observed toward a horizontal line that connects the stable gaseous density range with the stable liquid range rep-

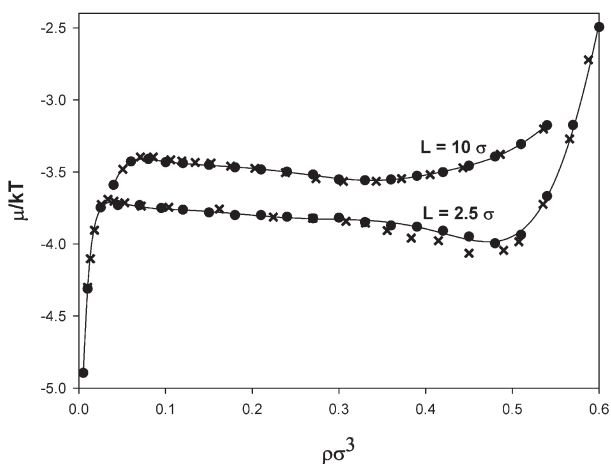


FIG. 1

Selected chemical potential versus density isotherms for the square-well fluid confined to hard planar slits. Upper curves:  $L = 10\sigma$ ,  $T^* = 1.05$ ; ● simulations of the large system with  $N = 567$ , × simulations of the small system with  $N = 343$ . Lower curves:  $L = 2.5\sigma$ ,  $T^* = 0.75$ ; ● simulations of the large system with  $N = 392$ , × simulations of the small system with  $N = 162$ . Full lines are numerical fits to Eq. (6)

representing the vapour/liquid coexistence chemical potential of an infinite system.

The calculation of the coexistence densities and chemical potentials is straightforward by numerically integrating the simulated subcritical  $\mu(\rho)$  isotherms according to the Maxwell-like equal-area construction discussed in the preceding section. Recently, we have calculated with this methodology coexistence data for the bulk square-well fluid<sup>4</sup> that we found to be in good overall agreement with the best-known literature data of del Rio et al.<sup>9</sup>. In the same paper we also estimated coexistence properties of planar monolayers, and we showed the consistency of the data with Gibbs ensemble simulations.

Table I shows the vapour/liquid coexistence densities and chemical potentials calculated from the above mentioned new chemical potential simulation data of confined fluids with wall separation distances of  $L = \{2.5\sigma, 6.0\sigma, 10.0\sigma\}$ . Additionally, in Table I there are shown coexistence data of the confined fluid with wall separation distance  $L = 4\sigma$ , recalculated from existing chemical potential data<sup>3</sup> using a polynomial fit of type Eq. (6).

Accounting for the observed significant particle number dependence of the subcritical  $\mu(\rho)$  loops, we have estimated also the vapour/liquid coexistence densities for a set of slit width  $L = \{2.5\sigma, 6.0\sigma, 10.0\sigma\}$  from the simulated isotherms with smaller numbers of particles  $N = \{162, 256, 343\}$ . We found, in contrast to the significantly changing  $\mu(\rho)$  loops, the differences in the estimated vapour/liquid coexistence densities and chemical potentials between the larger and the smaller system size studied, to be typically smaller than the expected numerical uncertainty of the data. This is in agreement with our general findings<sup>4</sup> that finite size effects on fluid phase equilibria of square-well fluids are usually weak, and particle numbers of several hundreds to about one thousand particles suffice to calculate accurately vapour/liquid equilibrium densities and the corresponding coexistence chemical potentials.

### *Critical Point Properties*

In order to calculate critical point properties of bulk and confined square-well fluids, we use both our new phase coexistence data of Table I and our recent data for bulk fluids and monolayers<sup>4</sup>. We exploit the scaling approach described in the last section, locating the critical point by nonlinear regression of the coexistence densities versus temperature data to the scaling ansatz (7), which describes the properties of the vapour/liquid densities

TABLE I

Vapour/liquid coexistence densities and chemical potentials for the square-well fluid confined in hard planar slits of different slit widths  $L$ . The precision of the data is estimated by comparing the results of Maxwell integrations with polynomials ( $\theta$ ) of different order and found to be typically 3–5% for the vapour density, and 1% for the liquid density, and 0.5% for the coexistence chemical potentials, respectively

$L, \sigma$	$N$	$T^*$	$\rho_v \sigma^3$	$\rho_l \sigma^3$	$\mu_{CO}/kT$
2.5	392	0.7250	0.0150	0.537	-4.032
		0.750	0.0198	0.523	-3.834
		0.7750	0.0270	0.508	-3.652
		0.8000	0.0376	0.492	-3.485
		0.8250	0.0517	0.472	-3.327
		0.8500	0.0745	0.442	-3.185
4.0	<i>a</i>	0.80	0.0121	0.522	-4.381
		0.90	0.0302	0.462	-3.727
		0.95	0.0481	0.430	-3.464
		1.00	0.0827	0.369	-3.241
6.0	500	0.975	0.0354	0.446	-3.667
		1.000	0.0431	0.430	-3.545
		1.025	0.0545	0.411	-3.430
		1.050	0.0688	0.389	-3.325
		1.075	0.0906	0.360	-3.227
10.0	567	1.0500	0.0483	0.423	-3.493
		1.0750	0.0593	0.405	-3.387
		1.1000	0.0721	0.384	-3.288
		1.1250	0.0889	0.357	-3.195
		1.1500	0.116	0.324	-3.107

<sup>a</sup> Results based on  $\mu(\rho)$  isotherms given in ref.<sup>3</sup> smoothed by improved polynomial fits.



in the vicinity of the critical point in terms of temperature difference to the critical point.

In Fig. 2 we demonstrate the influence of geometrical restrictions on the phase equilibria, showing both the temperature–density vapour/liquid phase diagrams and the corresponding critical points, calculated along these lines. Starting with the free bulk fluid, we show the increasing influence of the confinements by plotting the results for fluids confined to slits with decreasing width  $L = \{10\sigma, 6\sigma, 4\sigma, 2.5\sigma, 1\sigma\}$ , which includes the limiting case of planar monolayers.

Analyzing the coexistence densities, we observe that the confinement influence on the vapour phase is only weak, i.e., the density range of the vapour phase remains close to that of the bulk fluid with increasing geometrical restrictions for all confined systems studied, including the planar monolayer. In contrast to the vapour phase, the density of the liquid phase shows significant confinement effects. For wide slits in general the liquid range is shifted to lower densities, but narrowing the slit width towards the limit of monolayers, the liquid density range increases again and ap-

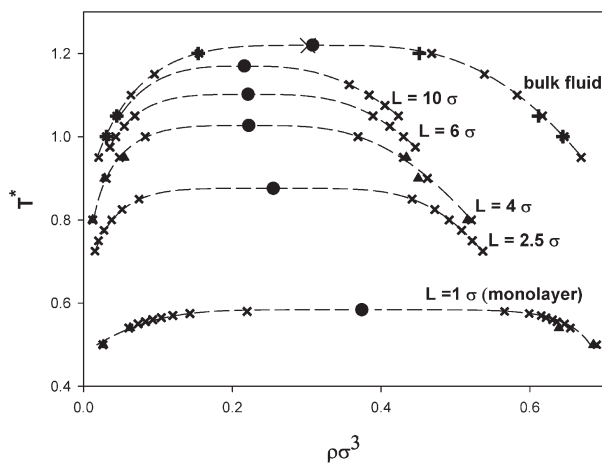


FIG. 2

Comparison of temperature–density vapour/liquid coexistence curves between the three-dimensional square-well fluid, and fluids confined in hard planar slits of slit widths  $L = \{2.5\sigma, 4.0\sigma, 6.0\sigma, 10\sigma\}$ , and planar two-dimensional layers ( $L = 1.0\sigma$ ).  $\times$  Simulation and Maxwell integration; --- scaling expression (7) adjusted to the coexistence densities;  $\bullet$  critical points from scaling expression (7); + literature data for coexistence densities of bulk square-well fluid<sup>9</sup>;  $\times$  literature data for critical point of bulk square-well fluid<sup>9</sup>;  $\blacktriangle$  independent Gibbs ensemble simulations for  $L = 4\sigma$  (ref.<sup>3</sup>) and  $L = 1\sigma$  (ref.<sup>4</sup>)

proaches, in the (two-dimensional) layer limit, the bulk liquid density range. The phase diagram of the layer looks quite similar to the bulk phase diagram, which is consistent with the interpretation of the monolayer as a free two-dimensional bulk fluid.

Some coexistence densities for square-well fluids in slit-like pores with widths between  $L = 4\sigma$  and  $16\sigma$  have been recently obtained by Shing and Kwak<sup>10</sup> using grand canonical MC. They show a figure with a temperature-density vapour/liquid phase diagram. Although they do not give explicitly numerical values, they report good mutual agreement of our previous results for  $L = 4\sigma$  (ref.<sup>3</sup>) with their grand canonical results. The phase diagram shown in ref.<sup>10</sup> is found to be consistent with the above discussed general confinement effects on the phase coexistence densities. Particularly, the observed significant lowering of the liquid phase density is confirmed by these data and found to be valid for wider slits, too.

TABLE II

Critical temperatures and densities and (effective) critical exponent  $\beta$  of the square-well fluid in the bulk and confined to hard planar slits of different widths  $L$  including the limiting case of planar two-dimensional layers ( $L = 1$ ) calculated by the use of scaling relation (7). The uncertainties of the results were estimated by sensitivity analysis of Eq. (7) in the same way as in ref.<sup>3</sup> The last digit error is given in parenthesis

$L, \sigma$	$N$	$T_C^*$	$\rho_c \sigma^3$	$\beta$
$\infty$ (bulk)	1000	1.220(4)	0.308(4)	0.280
10.0	567	1.170(3)	0.216(3)	0.342
6.0	500	1.102(3)	0.221(3)	0.278
4.0	500	1.027(4)	0.222(4)	0.271
2.5	392	0.876(3)	0.255(3)	0.200
1.0 (layer)	200	0.584(3)	0.374(3)	0.167 <sup>a</sup>
16.0	<i>b</i>	1.201	0.2082	
12.0	<i>b</i>	1.177	0.2143	
8.0	<i>b</i>	1.143	0.2101	
4.0	<i>b</i>	1.015	0.2265	

<sup>a</sup> Using a restricted temperature range very close to  $T_C$ , we find  $\beta = 0.127$ , close to the exact two-dimensional Ising model value of  $1/8$  (refs<sup>4,15</sup>). <sup>b</sup> Grand canonical MC results of Singh and Kwak<sup>10</sup>.

In agreement with general considerations<sup>1,2</sup> and previous studies<sup>3,10</sup>, we observe a significant decrease in the critical temperature with increasing geometrical restrictions, which will be discussed below in some detail.

The results of all our critical point calculations are summarized in Table II. We show not only the critical temperatures and densities but also the (effective) critical exponents  $\beta$ , obtained from Eq. (7). The critical exponent  $\beta$  for the planar monolayer is of special interest. If we identify this system with a two-dimensional square-well bulk fluid, we have to expect a value of the critical exponent of  $\beta = 1/8$ , which belongs to the corresponding two-dimensional Ising (lattice gas) model<sup>25</sup>. This can be verified by restricting our scaling procedure to a temperature range very close to the critical point, where, although the accuracy of our critical data calculation is limited by large fluctuations of the coexistence densities, the effective critical exponent approaches  $\beta \approx 0.127$ , which is very close to the expected analytical value of  $\beta = 1/8$  (for details, see ref.<sup>4</sup>).

For comparison, we have also included in Table II critical temperature and density results of Shing and Kwak<sup>10</sup>, which they obtained by scaling relations from their above discussed grand canonical MC simulations. In particular, for fluids confined to slits of width  $L = 4\sigma$ , the critical point data of Shing and Kwak can be compared directly with our results for the same slit width, showing the general agreement between our canonical results based on particle insertion and their grand canonical based results.

As mentioned before, our data show a strong suppression of the critical temperature with increasing confinement influence, i.e., with decreasing wall separation distance.

The results of a more detailed analysis of the shift of the critical temperature under confinement  $T_c^*$  with respect to the bulk critical temperature  $T_{cb}^*$  are presented in Fig. 3. For narrow slits, we found, in agreement with general considerations<sup>1,2</sup>, that the difference between the critical temperature of the bulk fluid and the confined fluid  $\Delta T_c^*$  decays approximately inversely proportional to the slit width  $L$

$$\Delta T_c^* \equiv T_{cb}^* - T_c^* \propto 1/L \quad (L \leq 10\sigma). \quad (8)$$

This relation is plotted as dashed line in Fig. 3. We can see that this simple relation is not able to describe accurately the limiting case of the planar layer and the properties of wide pores. To find a more general  $\Delta T_c^*$  versus  $L$  relation, that describes with reasonable accuracy besides narrow slits also

planar layers and wide pores, we introduced a simple exponential decaying function with an exponent reciprocal to a linear function in  $L$ .

$$\Delta T_c^* = a \exp [1/(bL + c)] \quad (9)$$

with constants  $a$ ,  $b$ ,  $c$ . Figure 3 shows the result of a nonlinear regression of all our critical temperature data for confined fluids, including monolayers to Eq. (9), treating the constants  $a$ ,  $b$ ,  $c$  as adjustable parameters. Plotting  $\Delta T_{\text{ex}}^*$  versus  $L$  according to Eq. (9) and comparing it with our simulation data, we find that the critical temperatures of all confined fluids studied – including the planar layers – can be described by Eq. (9), within the numerical uncertainties of the data. Additionally, we include in the figure the critical temperature results of the grand canonical MC simulations of Shing and Kwak<sup>10</sup> for fluids confined to several other slit widths, up to relatively wide slits with  $L = 16\sigma$ . These data are found to follow also our  $\Delta T_c^*(L)$  relation (9) with good accuracy, providing an independent check for the applicability of our proposed relation even to wider slits.

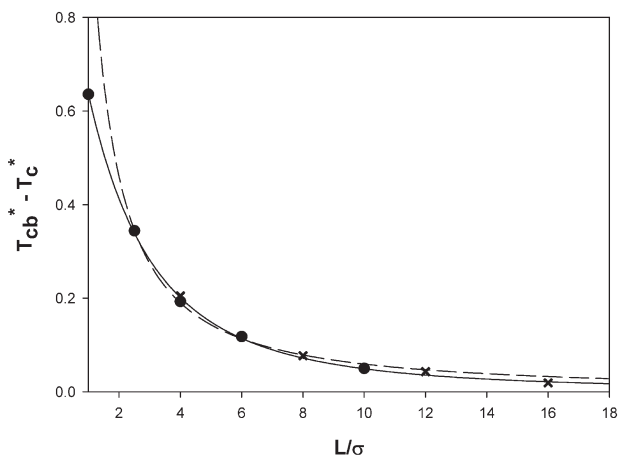


FIG. 3

Shift of the critical temperature for the square-well fluid  $\Delta T_c^* \equiv T_{\text{cb}}^* - T_c^*$  under the influence of confinement, modeling the transition from the three-dimensional bulk fluid to a two-dimensional monolayer via a series of hard slit-like pores with decreasing widths  $L$ . ● Results of this work, × results of Singh and Kwak<sup>10</sup>; - - - approximation for medium and narrow slits, Eq. (8); — Eq. (9), which describes accurately all existing critical point data

Considering the transition from the confined fluid to the bulk  $L \rightarrow \infty$ , Eq. (9) predicts an asymptotic decay, inversely proportional to  $L$ , for very large wall separation distances  $L$ . This is slightly different from the asymptotic decay of  $L^{-1/\nu}$  suggested by general scaling arguments, where  $\nu \approx 0.63$  is the critical exponent of the three-dimensional bulk fluid (for details, see ref.<sup>26</sup>). To investigate the exact asymptotic behaviour of the critical temperature shift of the square-well fluid by molecular simulation, one would need to study systematically a series of confined fluids with increasing wall separations, which are sufficiently large to permit the extrapolation to the  $L \rightarrow \infty$  limit. Such a study would require an extremely high demand on computer resources and the CPU time, and, therefore, goes beyond the scope of this paper.

### SUMMARY AND CONCLUSIONS

In this paper we have addressed the problem of the effect of geometrical restrictions on phase equilibrium properties of three-dimensional bulk square-well fluids. The restricting geometry is modeled to describe the transition from a three-dimensional to a two-dimensional bulk fluid by confining the fluid between two infinitely hard planar walls. An infinite large wall separation distance corresponds to the three-dimensional free bulk fluid. Decreasing the wall separation distance, we proceed via a series of hard slit-like pores to a planar monolayer of square-well molecules, which is equivalent to a two-dimensional bulk square-well fluid.

To study the corresponding phase equilibria, we applied to both the bulk and confined fluids a recently proposed methodology<sup>3</sup>, which combines MC simulations of chemical potential versus density isotherms in the subcritical vapour/liquid two phase range with thermodynamic integration of these isotherms to obtain vapour/liquid coexistence densities and chemical potentials by a Maxwell-like equal area integration.

In order to investigate the confinement influence on phase equilibrium properties, we used both existing coexistence data estimated along these lines in our previous papers<sup>3,4</sup> and we simulated new sets of subcritical chemical potential isotherms for several slit widths and calculated the corresponding coexistence properties.

We describe the temperature–density vapour/liquid coexistence curves by simple scaling relations of the type of Eq. (7) and determine the corresponding critical temperatures, densities, and (effective) critical exponents by linear regression to the vapour/liquid coexistence density. In agreement with literature data<sup>10</sup>, we found different properties of the equilibrium den-

sities of the coexisting fluid phases under confinement. While in general the density range of the vapour phase does not much change due to geometrical restrictions, the density range of the liquid phase is significantly lower than that of the three-dimensional bulk liquid. In this paper we extended such studies for the first time to very narrow slits and monolayers and we found a significant increase in the liquid density with decreasing wall separation distance. In the limiting case of the planar monolayer the phase diagram looks qualitatively quite similar to that of the free bulk fluid. This supports the identification of the monolayer with a two-dimensional bulk fluid.

As expected, we observed a significant suppression of the critical temperature with increasing geometrical restrictions. For medium to narrow wall separation distances, we found the expected<sup>1,2</sup> critical temperature shift approximately inversely proportional to the slit width.

In this work we proposed a more general expression Eq. (9), which exponentially decays in terms of the reciprocal slit width. We proved that the new equation is able to describe accurately all existing critical temperature shift data for a wide range of wall separation distances, reaching from fluids confined to wide slits with wall separation distance of  $L = 16\sigma$  to very narrow slits and even planar fluid monolayers (two-dimensional bulk square-well fluids).

In general, the presented new results, describing the influence of geometrical restrictions on fluid phase equilibria and critical properties, contribute to a more detailed molecular-based understanding of phase equilibria not only for simple square-well fluids but also for more complex molecular fluids with square-well interactions involved.

Summarizing the results of this and our previous studies<sup>3-6</sup>, we found the proposed combination of particle insertion MC methods with thermodynamic integration to be conceptionally simple, easy to implement in existing canonical simulation codes, and capable of providing reliable phase equilibria data for both free bulk and confined fluids. Taking into account the increase in efficiency of the chemical potential simulations by the use of improved particle insertion strategies<sup>5,6,14,16</sup>, we consider the proposed methodology to be an interesting alternative route to grand canonical or Gibbs ensemble simulations of phase equilibrium properties of fluids.

*The author thanks Dr Matthias Kettler, Leipzig, for helpful discussions.*

## REFERENCES

1. Evans R.: *J. Phys., Condens. Matter* **1990**, *2*, 8989.
2. Gelb L. D., Gubbins K. E., Radhakrishnan R., Sliwinska-Bartkowiak M.: *Rep. Prog. Phys.* **1999**, *62*, 1573.
3. Vörtler H. L., Smith W. R.: *J. Chem. Phys.* **2000**, *112*, 5168.
4. Vörtler H. L., Schäfer K., Smith W. R.: *J. Phys. Chem. B* **2008**, *112*, 4656.
5. Vörtler H. L., Kettler M.: *Chem. Phys. Lett.* **2003**, *377*, 557.
6. Vörtler H. L., Kettler M.: *Mol. Phys.* **2006**, *104*, 233.
7. Yethiraj A., Hall C. K.: *J. Chem. Phys.* **1991**, *95*, 1999.
8. Nezbeda I., Slovak J.: *Mol. Phys.* **1997**, *90*, 353.
9. del Rio F., Avalos E., Espindola R., Rull L. F., Jackson G., Lago S.: *Mol. Phys.* **2002**, *100*, 2531.
10. Singh J. K., Kwak S. K.: *J. Chem. Phys.* **2007**, *126*, 024702.
11. Allen M. P., Tildesley D. J.: *Computer Simulations of Liquids*. Clarendon, Oxford 1987.
12. Frenkel D., Smit B.: *Understanding Molecular Simulation: From Algorithms to Applications*. Academic Press, San Diego 2002.
13. Widom B.: *J. Chem. Phys.* **1963**, *39*, 2808.
14. Tripathi S., Chapman W. G.: *Mol. Phys.* **2003**, *101*, 1199.
15. Schäfer K.: *M.S. Thesis*. Universität Leipzig, Leipzig 2006.
16. Labik S., Malijevsky A., Kao R., Smith W. R., del Rio F.: *Mol. Phys.* **1999**, *96*, 849.
17. Widom B.: *J. Stat. Phys.* **1978**, *19*, 563.
18. Flyvbjerg H., Peterson H. G.: *J. Chem. Phys.* **1989**, *91*, 461.
19. Wegner F. J.: *Phys. Rev. B* **1972**, *5*, 4529.
20. Green D. G., Jackson G.: *J. Chem. Phys.* **1994**, *101*, 3190.
21. Vega L., de Miguel E., Rull L. F., Jackson G., McLure I. A.: *J. Chem. Phys.* **1992**, *96*, 2296.
22. Furukawa H., Binder K.: *Phys. Rev. A* **1982**, *26*, 556.
23. MacDowell L. G., Virnau P., Müller M., Binder K.: *J. Chem. Phys.* **2004**, *120*, 5293.
24. MacDowell L. G., Chen V. K., Errington J. R.: *J. Chem. Phys.* **2006**, *125*, 034705.
25. Chandler D.: *Introduction to Modern Statistical Mechanics*. Oxford University Press, Oxford 1987.
26. Fisher M., Nakanishi H.: *J. Chem. Phys.* **1981**, *75*, 5857.